



# Density functional theory study of the near edge X-ray absorption fine structure and infrared spectroscopy of acetylene and benzene on group IV semiconductor surfaces

Frans A. Asmuruf, Nicholas A. Besley\*

School of Chemistry, University of Nottingham, University Park, Nottingham NG7 2RD, UK

## ARTICLE INFO

### Article history:

Received 10 July 2008

Accepted for publication 29 October 2008

Available online 9 November 2008

### Keywords:

Infrared spectroscopy

NEXAFS

DFT

Acetylene

Benzene

## ABSTRACT

The near edge X-ray absorption fine structure and infrared spectroscopy of acetylene and benzene adsorbed on C(100)-2 × 1, Si(100)-2 × 1 and Ge(100)-2 × 1 surfaces is studied with density functional theory calculations. Time dependent density functional theory calculations of the near edge X-ray absorption fine structure with a modified exchange-correlation functional agree well with experiment, and show that the spectral features arise from excitation to  $\pi^*$ ,  $\sigma_{C-H}^*$  and  $\sigma_{X-C}^*$  orbitals, where X represents C, Si or Ge. The  $\sigma_{X-C}^*$  excitation energies are dependent on the surface, and for acetylene, the location of the  $\pi^*$  band also varies with the surface. Calculations of the vibrational modes show the C–H stretching frequencies for carbon atoms bonded directly to the surface vary significantly between the three surfaces, while those for carbon atoms not bonded to the surface do not change significantly.

© 2008 Elsevier B.V. All rights reserved.

## 1. Introduction

The study of hydrocarbon chemistry on semiconductor surfaces has been the focus of considerable attention in recent years. This interest is in part motivated by the importance of these systems in emerging technologies [1]. Problems that have been addressed include the reaction of organic molecules with the surface, and the structure of the resulting adsorbed molecule. Most of this work has focused on the Si(100)-2 × 1 surface. Detailed studies have been reported for a wide range of molecules, from small molecules such as butadiene [2–4] to much larger systems such as C<sub>60</sub> [5–7]. In comparison to Si(100)-2 × 1, the related Ge(100)-2 × 1 and C(100)-2 × 1 surfaces have received much less attention. However, several studies have been reported, and much of this work has been reviewed elsewhere [1,8,9]. Hydrocarbons adsorbed on Ge(100)-2 × 1 reveal similar chemistry to the reactions on Si(100)-2 × 1, but the products are less strongly bound due to the weaker C–Ge bond [10,11]. The structure of acetylene on Si(100)-2 × 1 has been studied by a number of groups [12–14]. Recent work has used multireference wavefunctions with dynamic correlation [15]. This work found the most stable binding site to correspond to acetylene bonded to a single surface dimer, with an acetylene carbon–carbon bond length of 1.36 Å. A comprehensive investigation of benzene adsorbed on the Si(100)-2 × 1 surface has been reported, and showed that the favoured binding

site to correspond to the butterfly structure arising from a 4 + 2 addition [16]. Density functional theory (DFT) calculations have been used to study the adsorption of acetylene and benzene on the Ge(100)-2 × 1 surface [17]. These calculations were consistent with the observation that there is a weaker binding to the Ge(100)-2 × 1 surface. Theoretical studies have also investigated the adsorption of several small molecules, such as acetylene, the methyl radical and carbon dimer on diamond surfaces [18–22].

Spectroscopic measurements, often in concert with theoretical calculations, can allow the structure of the adsorbed species to be determined, and infrared (IR) and near edge X-ray adsorption fine structure (NEXAFS) spectroscopies have been used extensively to probe molecules adsorbed on the Si(100)-2 × 1 surface. In this paper, the sensitivity of the spectroscopy of an adsorbed unsaturated organic molecule to the nature of the underlying surface is studied. Acetylene and benzene are used as model systems, and their NEXAFS and IR spectroscopy on the C(100)-2 × 1, Si(100)-2 × 1 and Ge(100)-2 × 1 surfaces is computed using DFT.

NEXAFS measures the excitation of core electrons to semi-stable states below the ionization threshold. Several groups have reported NEXAFS studies of acetylene and benzene on Si(100)-2 × 1. In a study of acetylene on the Si(100)-2 × 1 surface, Matsui and co-workers observed peaks at 284.7, 286.0 and 287.6 eV, which were assigned to excitations from the carbon 1s orbitals to  $\pi_{C-C}^*$ ,  $\sigma_{Si-C}^*$  and  $\sigma_{C-H}^*$  orbitals, respectively [23,24]. Above threshold, a broad peak at 300 eV was observed and assigned to the  $\sigma_{C-C}^*$  orbital. In a later study, Pietzsch et al. reported a fully polarization resolved NEXAFS investigation of acetylene on the surface [25].

\* Corresponding author. Tel.: +44 115 951 3474; fax: +44 115 951 3562.  
E-mail address: [nick.besley@nottingham.ac.uk](mailto:nick.besley@nottingham.ac.uk) (N.A. Besley).

Acetylene adsorbed on the surface showed four resonances at 283.8, 286.7, 288.4 and 299 eV, in broad agreement with earlier work. Interestingly, the  $\pi_{\text{C-C}}^*$  feature was evident in spectra with the incident radiation parallel or perpendicular to surface silicon dimers, indicating that two adsorption products are present.

NEXAFS spectra of benzene adsorbed on Si(100)-2 × 1 have been reported by Kong et al. [26]. At 100 K benzene is predominantly physisorbed to the surface and the resulting spectra have two peaks at 285.0 and 288.8 eV due to C(1s) →  $\pi^*(e_{2u})$  and C(1s) →  $\pi^*(b_{2g})$  transitions. In contrast, at room temperature chemisorption is favoured. The  $\pi^*$  excitation was found at 285 eV, with weaker bands at 287.7 and 289.5 eV arising from excitation to  $\sigma_{\text{C-H}}^*$  and  $\sigma_{\text{Si-C}}^*$  orbitals. In polarized NEXAFS measurements for benzene, the  $\pi^*$  feature was evident at more than one polarization, indicating that benzene is no longer flat on adsorption [27]. The application of NEXAFS to study Ge(100)-2 × 1 and C(100)-2 × 1 is much less common. Studies of sulphur atoms adsorbed on Ge(100)-2 × 1 [28], and hydrogenated C(100)-2 × 1 surface [29] have been reported, but to our knowledge the NEXAFS of acetylene or benzene on these surface has not been measured. Time dependent density functional theory (TDDFT) calculations of the NEXAFS of acetylene and benzene have also been reported [30]. A modified exchange–correlation functional in which the fraction of Hartree–Fock exchange was optimized was used in conjunction with the 6-31 + G\* basis set. In general, the calculations were in good agreement with experiment, particularly for the valence states. For benzene the location of the dominant  $\pi_{\text{C-C}}^*$  band was found to be sensitive to the adsorption geometry.

IR spectroscopy is a particularly powerful technique to study the products of reactions on semiconductor surfaces. For the reaction of unsaturated hydrocarbons, these studies have focused on the C–H stretching region of the spectrum. The IR spectrum of benzene deposited on Si(100)-2 × 1 at 100 K has been reported [26]. Strong IR absorption peaks were observed at 3086, 3067, 3036, and 3030 cm<sup>-1</sup> which correspond to the vibrational features of molecular benzene, and the adsorption product was subsequently identified as physisorbed benzene. For benzene chemisorbed on the surface, the hybridization of the carbons directly bonded to the surface change from sp<sup>2</sup> to sp<sup>3</sup>. At room temperature benzene is chemisorbed on the surface and two peaks at 3044 and 2945 cm<sup>-1</sup> are observed, and assigned to the C–H stretching of the sp<sup>2</sup> and sp<sup>3</sup> hybridized carbons, respectively. This was consistent with earlier work [31]. Another study showed several C–H stretching bands in the frequency range 2899–3043 cm<sup>-1</sup>, and determined the dominant adsorption product to correspond to a 1,4-cyclohexadiene like structure [32]. More recently, the vibrational spectroscopy of benzene was re-examined. Three different chemisorbed phases were identified, which corresponded to the 1,4-cyclohexadiene structure but bonded to a single Si–Si dimer or bridging between two dimers [33]. Measurements of the IR spectrum of ethylene on Ge(100)-2 × 1 showed the symmetric and antisymmetric C–H stretching modes to occur at 2913 and 2961 cm<sup>-1</sup>, respectively [11].

A number of theoretical calculations of vibrational frequencies of the organic molecules on the Si(100)-2 × 1 surface have been reported [2,3,34–38]. These calculations usually use DFT and adopt small cluster models of the surface, however, larger surface clusters have been using in conjunction with semi-empirical calculations [32]. The vibrational frequencies of acetylene on the Si(100)-2 × 1 surface computed at the MCSCF + MRMP2 level of theory [15]. Recently, a partial Hessian approach was employed to compute the IR spectroscopy of a range of organic molecules, including acetylene and benzene, on Si(100)-2 × 1 using DFT [39]. The adoption of the partial Hessian methodology reduced the cost of the calculations and allowed larger cluster models of the surface to be used.

## 2. Computational details

TDDFT is well established for computing valence excited states. Core excitations are dominated by single excitations and should be described well by TDDFT, and TDDFT has been extended to the efficient computation of core excited states [40,30]. Within the Tamm–Dancoff approximation (TDA) [41] of TDDFT, excitation energies and oscillator strengths are determined as the solutions to the eigenvalue equation [42]

$$\mathbf{AX} = \omega\mathbf{X} \quad (1)$$

The matrix  $\mathbf{A}$  is given by

$$A_{ia,jb} = \delta_{ij}\delta_{ab}(\varepsilon_a - \varepsilon_i) + (ia|jb) + (ia|f_{\text{xc}}|jb) \quad (2)$$

where two-electron integrals are given in Mulliken notation,

$$(ia|f_{\text{xc}}|jb) = \int d\mathbf{r}d\mathbf{r}' \psi_a^*(\mathbf{r})\psi_i(\mathbf{r}) \frac{\delta^2 E_{\text{xc}}}{\delta\rho(\mathbf{r})\delta\rho(\mathbf{r}')} \psi_j^*(\mathbf{r}')\psi_b(\mathbf{r}) \quad (3)$$

and the convention of  $i, j, \dots$  denoting occupied orbitals and  $a, b, \dots$  denoting virtual orbitals is adopted.  $\mathbf{X}$  describes the linear response of the Kohn–Sham density matrix in the basis of the unperturbed molecular orbitals,  $\varepsilon_i$  are the orbital energies,  $\omega$  give the excitation energies and  $E_{\text{xc}}$  is the exchange–correlation functional.

The calculation of core excited states with standard TDDFT implementations is inefficient because of the large number of roots of Eq. (1) that are required. A solution to this problem is to perform the TDDFT calculation within the subspace of single excitations involving excitations from the relevant core orbital(s). The following equation is solved [40,43]

$$\bar{\mathbf{A}}\mathbf{X} = \omega\mathbf{X} \quad (4)$$

where

$$\bar{\mathbf{A}} = A_{i\bar{i},j\bar{j}} \quad (5)$$

and  $\{\bar{i}\}$  represents a subset of the occupied orbitals. For core excitations, this approximation introduces a very small error in the computed excitation energies [44]. We have used this approach to study the NEXAFS [30,44] and electronic [45,46] spectroscopy of a variety of molecules adsorbed on surfaces. For the systems studied here, electronic excitations from the two carbon 1s orbitals of acetylene and the six carbon 1s orbitals of benzene to the entire virtual space are included in the excitation space.

Core excitation energies computed with TDDFT show a large underestimation, which increases with the nuclear charge of the atom on which the core orbital is localized. Consequently, while the spectra are often correct, they need to be shifted in energy to match experiment. The origin of this error is associated with the approximate local exchange used in most exchange–correlation functionals. One way to address this problem is to adjust the proportion of Hartree–Fock exchange in the hybrid functional [47,48,30]. In this work, a modified hybrid exchange–correlation functional is used with an increased fraction of Hartree–Fock exchange [30].

$$\text{BH}^{0.57}\text{LYP} = 0.57\text{HF} + 0.35\text{B} + 0.08\text{S} + 0.81\text{LYP} + 0.19\text{VWN} \quad (6)$$

where HF, B and S are Hartree–Fock, Becke [49] and Slater [50] exchange functionals, respectively, and LYP [51] and VWN [52] are correlation functionals. This functional has been designed to predict correctly the core excitation energies for carbon 1s excitations, but is also accurate for core excitations from the 1s orbitals of other first row atoms. A mixed basis set comprising the 6-311++G\* basis set for the atoms of the adsorbed molecule and the 6-311G\* basis set for the atoms of the surface cluster was used. C<sub>9</sub>H<sub>12</sub>, Si<sub>9</sub>H<sub>12</sub> and Ge<sub>9</sub>H<sub>12</sub> clusters are used to model the surfaces, and molecules are treated as binding to one surface dimer, with “butterfly” binding

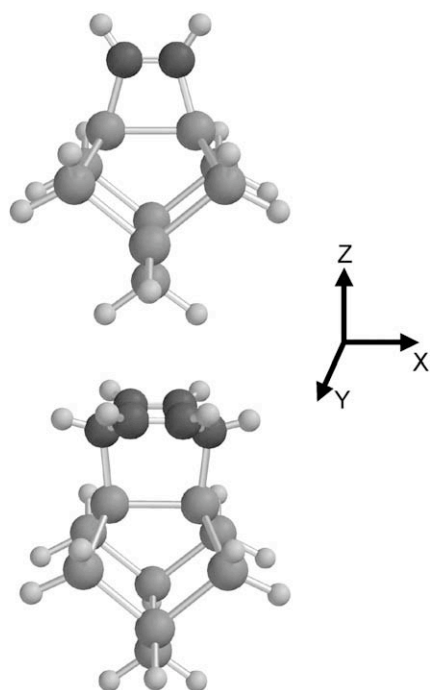


Fig. 1. Models of acetylene and benzene adsorbed on the Si(100)-2 × 1 surface.

configurations considered for benzene. These binding configurations are often referred to as the “di-σ” structure and have been shown to be the favored binding site for acetylene and benzene on Si(100)-2 × 1 and Ge(100)-2 × 1 [53,17]. Structures were optimized at the B3LYP/6-31G\* level of theory, and Fig. 1 shows acetylene and benzene bound to the Si<sub>9</sub>H<sub>12</sub> surface cluster. Spectra are generated by representing each computed core excitation and associated intensity with a Gaussian function with full width at half maximum of 0.3 eV.

Within the harmonic approximation, vibrational frequencies and normal modes are obtained from diagonalization of the mass-weighted Hessian matrix, with the associated intensities evaluated through the derivative of the dipole moment with respect to the normal coordinates. In this work, a partial Hessian methodology is adopted [54,55] in which the Hessian matrix is truncated to include the energy derivatives associated with the adsorbed molecule and the two surface atoms bonded to the adsorbate. Earlier work has shown that this approximation introduces a small error in the computed vibrational properties, particularly for the C–H stretching modes, and yields a substantial reduction in computational expense [39]. The single dimer surface cluster models are also used for the IR calculations. For the vibrational frequency calculations the B3LYP functional was used in conjunction with the 6-311G\*\* basis set. The exception was for the Ge(100)-2 × 1 surface, where to reduce the cost of the calculation, the 6-31G\* basis set was used for the atoms of the surface cluster not bonded to the adsorbant. The structures were fully optimized at the same level of theory prior to the frequency calculations, and the resulting vibrational frequencies are scaled by the standard factor of 0.96 [56]. All calculations were performed with a development version of the Q-Chem software package [57].

### 3. Results and discussion

#### 3.1. Near edge X-ray absorption fine structure

Fig. 2 shows the computed x,y and z-polarized NEXAFS spectra for acetylene adsorbed on the surfaces. The computed spectrum

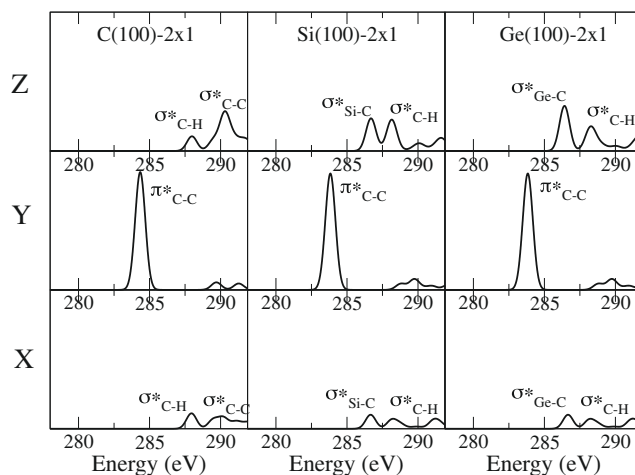


Fig. 2. Computed BH<sup>0.57</sup>LYP x,y and z-polarized spectra for acetylene adsorbed on C(100)-2 × 1, Si(100)-2 × 1 and Ge(100)-2 × 1.

for acetylene on Si(100)-2 × 1 is similar to previous work [30], although a different basis set is used here. The spectrum is dominated by an intense transition that appears with y polarization. This corresponds to excitation to the  $\pi_{C-C}^*$  orbital, which is shown in Fig. 3. At higher energy, weaker bands are evident in the x and z polarized spectra. These correspond to excitation to  $\sigma_{Si-C}^*$  and  $\sigma_{C-H}^*$  orbitals, these orbitals are also shown in Fig. 3. This is consistent with experiment, the  $\pi_{C-C}^*$ ,  $\sigma_{Si-C}^*$  and  $\sigma_{C-H}^*$  bands are observed at 284.7, 286.0 and 287.6 eV [23,24], respectively, which compare well with the computed values of 283.8, 286.7 and 288.2 eV, and indicates that the modified hybrid exchange–correlation functional used provides a good description of these excitations.

The predicted spectra for acetylene on the C(100)-2 × 1 and Ge(100)-2 × 1 surfaces appear similar, although there is variation in the position of the spectral bands. Table 1 summarizes the computed excitation energies on the three surfaces. The C(1s) →  $\pi_{C-C}^*$  excitation energy is dependent on the surface, and increases in the order Si(100)-2 × 1 < Ge(100)-2 × 1 < C(100)-2 × 1. This ordering can be rationalized by the C–C bond length of the adsorbed acetylene molecule. This bond length is shortest on the C(100)-2 × 1 surface and longest on the Si(100)-2 × 1 surface. Shortening of the C–C bond length will lead to a destabilization of the  $\pi_{C-C}^*$  orbital, and result in an increase in the associated core excitation energy. There is little change in the computed excitation energy for the C(1s) →  $\sigma_{C-H}^*$  excitation. This is reasonable since the  $\sigma_{C-H}^*$  orbital is located on the carbon and hydrogen of the acetylene molecule, and has little interaction with the surface. The  $\sigma_{X-C}^*$  (where X denotes C, Si or Ge) orbital has a large contribution from the surface, and the associated excitation is the most sensitive to the surface. The excitation energy is much higher for the C(100)-2 × 1 surface, and results in a change in the order of the  $\sigma_{C-H}^*$  and  $\sigma_{X-C}^*$  bands. In the z-polarized spectrum, the  $\sigma_{C-C}^*$  band forms part of a larger band, which has its maximum at a slightly higher energy than the value of 289.5 eV recorded in Table 1. The higher energy of the  $\sigma_{C-C}^*$  band on the C(100)-2 × 1 surface is likely to be a consequence of the greater strength of the adsorbate–surface C–C bonds compared to Si–C and Ge–C bonds.

It is interesting to compare the spectra computed with the BH<sup>0.57</sup>LYP functional with the more standard B3LYP functional. Fig. 4 shows NEXAFS spectra for acetylene on the three surfaces computed with the B3LYP functional and the computed excitation energies for the  $\pi_{C-C}^*$ ,  $\sigma_{C-H}^*$  and  $\sigma_{X-C}^*$  excitations are shown in Table 1. It is well known that the B3LYP functional underestimates core excitation energies for carbon 1s excitations by about 10 eV, and this is observed for the excitations considered here. However, the

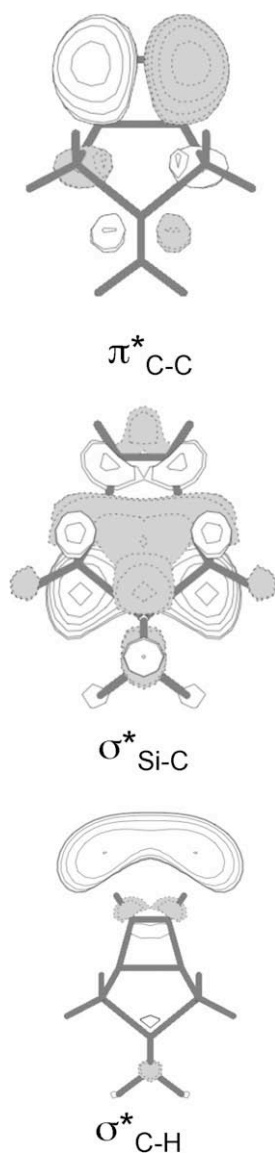


Fig. 3. Virtual orbitals of acetylene adsorbed on Si(100)-2 × 1.

Table 1

Computed excitation energies and C–C bond lengths of acetylene adsorbed on the surfaces. Experimental results for the Si(100)-2 × 1 surface [23,24].

Surface	$\pi_{C-C}^*$ (eV)	$\sigma_{C-H}^*$ (eV)	$\sigma_{X-C}^*$ (eV)	$r_{C-C}$ (Å)
<i>BH<sup>0.57</sup>LYP</i>				
C(100)-2 × 1	284.3	288.0	289.5	1.340
Si(100)-2 × 1	283.8	288.2	286.7	1.352
Ge(100)-2 × 1	284.1	288.1	286.4	1.344
<i>B3LYP</i>				
C(100)-2 × 1	274.4	276.1	279.3	1.340
Si(100)-2 × 1	273.8	276.5	274.9	1.352
Ge(100)-2 × 1	274.1	276.4	274.9	1.344
Experiment	284.7	287.6	286.0	

spectra are qualitatively similar to the spectra obtained with the BH<sup>0.57</sup>LYP functional. The main differences between the two functionals are in the intensities of some bands, and the energy separation between the  $\pi_{C-C}^*$  band and the higher energy bands is smaller for the B3LYP functionals. Detailed analysis of the excitation ener-

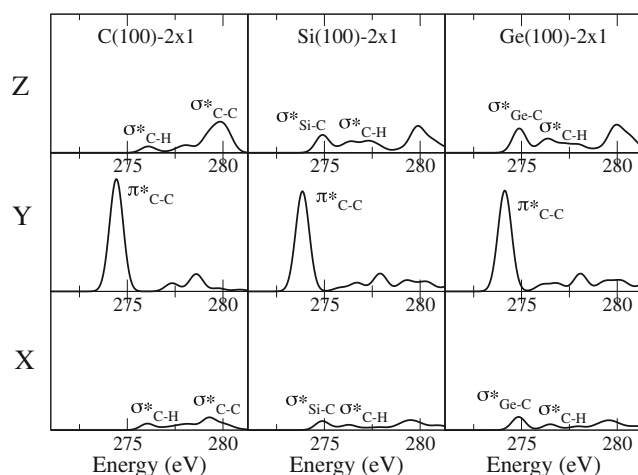


Fig. 4. Computed B3LYP *x,y* and *z*-polarized spectra for acetylene adsorbed on C(100)-2 × 1, Si(100)-2 × 1 and Ge(100)-2 × 1.

gies show similar trends to those observed for the BH<sup>0.57</sup>LYP functional. For example, the C(1s) →  $\pi_{C-C}^*$  excitation energy increases in the order Si(100)-2 × 1 < Ge(100)-2 × 1 < C(100)-2 × 1, there is little change in the computed excitation energy for the C(1s) →  $\sigma_{C-H}^*$  excitation between the three surfaces and the  $\sigma_{X-C}^*$  excitation is much higher for the C(100)-2 × 1 surface.

Fig. 5 shows the computed spectra for benzene adsorbed on the three surfaces. Several bands are observed in the spectra, which correspond to excitation to  $\pi^*$ ,  $\sigma_{C-H}^*$  and  $\sigma_{X-C}^*$  orbitals. These orbitals are shown for the Si(100)-2 × 1 surface in Fig. 6. For the Si(100)-2 × 1 surface excitation to the  $\pi^*$  orbitals results in an intense band in the *z*-polarized spectrum. A weaker  $\pi^*$  band is also observed in the *y*-polarized spectrum indicating that benzene is no longer planar on adsorption. The  $\pi^*$  band of benzene on Si(100) is computed to lie at 284.6 eV, which agrees well with the value of 284.8 eV measured in experiment [27]. An additional feature at 286.9 eV was also observed in experiment. The calculations show two further bands at higher energies corresponding to excitation to  $\sigma_{Si-C}^*$  and  $\sigma_{C-H}^*$  orbitals, and are computed to lie at 286.8 eV and 287.9 eV. Based on these results, the additional band observed in experiment corresponds to the  $\sigma_{Si-C}^*$  excitation, although this does not agree with assignments made in earlier experimental work [26].

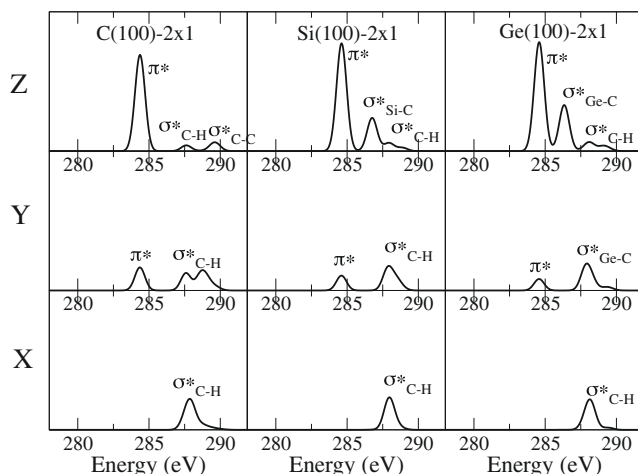


Fig. 5. Computed BH<sup>0.57</sup>LYP *x,y* and *z*-polarized spectra for benzene adsorbed on C(100)-2 × 1, Si(100)-2 × 1 and Ge(100)-2 × 1.

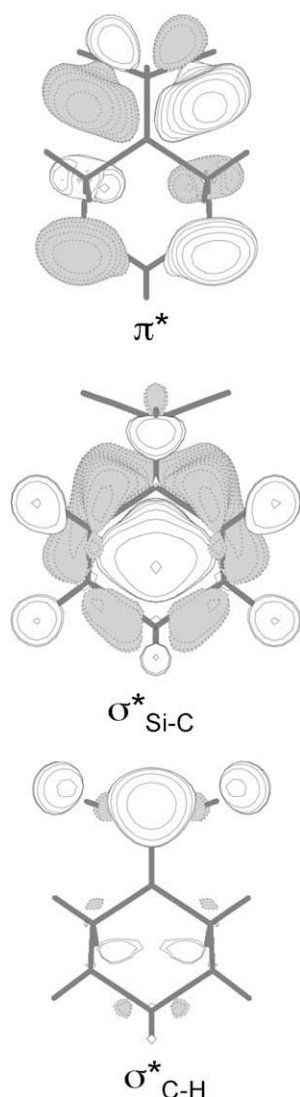


Fig. 6. Virtual orbitals of benzene adsorbed on Si(100)-2  $\times$  1.

The excitation energies for benzene on the three surfaces are summarized in Table 2. Unlike acetylene, the  $\pi^*$  excitation energies do not show a dependence on the surface. This is physically intuitive since the  $\pi^*$  orbitals are associated with the  $sp^2$  carbons that are not bonded directly to the surface (see Fig. 6), and as a result will not be affected by the change of surface to the same extent. The  $\sigma_{C-H}^*$  and  $\sigma_{Si-C}^*$  excitations show a similar behavior to that observed for acetylene. The  $\sigma_{C-H}^*$  is localized on the benzene molecule, and the corresponding excitation energy does not vary significantly between the three surfaces. The  $\sigma_{Si-C}^*$  excitation is significantly higher for the C(100)-2  $\times$  1 surface, and results in a change in the order of the  $\sigma_{C-H}^*$  and  $\sigma_{Si-C}^*$  bands.

Table 2

Computed excitation energies of benzene adsorbed on the surfaces. Experimental results for the Si(100)-2  $\times$  1 surface [27].

Surface	$\pi_{C-C}^*$ (eV)	$\sigma_{C-H}^*$ (eV)	$\sigma_{Si-C}^*$ (eV)
C(100)-2 $\times$ 1	284.4	287.6	289.6
Si(100)-2 $\times$ 1	284.6	287.9	286.8
Ge(100)-2 $\times$ 1	284.6	287.8	286.3
Experiment	284.5	–	286.9

### 3.2. Infrared spectroscopy

Experimental measurements of the IR spectroscopy of organic molecules adsorbed on semiconductor surfaces focus on the C–H stretching region, and in this work we will also concentrate on these vibrational modes. For the C(100)-2  $\times$  1 and Si(100)-2  $\times$  1 surface clusters used in this study, harmonic frequency calculations using the full Hessian can be performed. However, for the Ge(100)-2  $\times$  1 surface, the calculation of the vibrational frequencies becomes computationally expensive. Therefore, it is quite useful to adopt a partial Hessian framework to reduce the cost of these calculations, and for consistency this approach is used for all three surfaces. The partial Hessian approximation for vibrational frequencies is analogous to the assumption that atoms not included in the Hessian matrix have infinite mass. Earlier work showed that this approximation introduced a very small error for the C–H stretching modes of organic molecules on the Si(100)-2  $\times$  1 surface [39]. Since carbon is lighter than silicon, it is necessary to examine the partial Hessian approximation for the adsorbants on the C(100)-2  $\times$  1 surface. For acetylene on the C(100)-2  $\times$  1 surface, a full Hessian calculation predicts the symmetric C–H and antisymmetric C–H stretching vibrations to have (unscaled) frequencies of 3183.7  $cm^{-1}$  and 3152.3  $cm^{-1}$  with associated intensities 49.0  $km\ mol^{-1}$  and 18.4  $km\ mol^{-1}$ , respectively. This compares with 3183.7  $cm^{-1}$  and 3152.3  $cm^{-1}$  with intensities 49.8  $km\ mol^{-1}$  and 17.4  $km\ mol^{-1}$  for the partial Hessian calculation. Thus, even for the C(100)-2  $\times$  1 surface, the partial Hessian approximation introduces essentially no error for the computed frequencies and a very small change in the computed intensities. For the Si(100)-2  $\times$  1 surface the unscaled vibrational frequencies for the symmetric C–H, antisymmetric C–H and C–C stretching mode are 3128.6, 3105.6 and 1572.0  $cm^{-1}$ . These can be compared to corresponding frequencies of 3324, 3302 and 1575  $cm^{-1}$  computed at the MCSCF + MRMP2 level of theory [15]. This shows the C–H stretching frequencies to be significantly lower in the present calculations.

Table 3 shows the computed frequencies of the relevant vibrational modes. For acetylene, the C–H stretching region of the spectrum shows an intense band corresponding to the symmetric stretching mode and a weak band corresponding to the antisymmetric stretch. There is only a small difference of approximately 5  $cm^{-1}$  between the computed frequencies on the Si(100)-2  $\times$  1 and Ge(100)-2  $\times$  1 surface, but for the C(100)-2  $\times$  1 surface the predicted frequencies are significantly higher. This is consistent with experimental measurements of C–H stretching modes of butadiene, which found a difference of less than 15  $cm^{-1}$  between Si(100)-2  $\times$  1 and Ge(100)-2  $\times$  1 surfaces [10]. Another mode of interest is the C–C stretch, the computed frequencies increase in the order Si(100)-2  $\times$  1 < Ge(100)-2  $\times$  1 < C(100)-2  $\times$  1. This is

Table 3

Computed vibrational frequencies (in  $cm^{-1}$ ) and intensities (in  $km\ mol^{-1}$ ) for the C–H stretching modes. Frequencies have been scaled by 0.96. Experimental results from reference [26].

Mode	C(100)-2 $\times$ 1	Si(100)-2 $\times$ 1	Ge(100)-2 $\times$ 1	Experiment (Si(100)-2 $\times$ 1)
<i>Acetylene</i>				
Symmetric C–H	3056.3 (49.8)	3003.5 (65.4)	3009.8 (62.3)	
Antisymmetric C–H	3026.2 (17.4)	2981.4 (6.1)	2985.3 (3.5)	
C–C stretch	1606.6 (2.8)	1509.1 (0.5)	1520.8 (5.2)	
<i>Benzene</i>				
C–H stretch ( $sp^2$ )	3069.0 (16.2)	3065.1 (13.7)	3062.2 (16.3)	3044
C–H stretch ( $sp^2$ )	3066.3 (20.6)	3062.7 (16.2)	3059.6 (18.1)	
C–H stretch ( $sp^2$ )	3045.4 (14.4)	3044.0 (3.9)	3041.7 (5.2)	
C–H stretch ( $sp^2$ )	3044.0 (0.0)	3042.8 (0.0)	3040.2 (0.0)	
C–H stretch ( $sp^3$ )	2957.7 (0.6)	2971.9 (6.3)	2993.4 (7.4)	2945
C–H stretch ( $sp^3$ )	2958.0 (62.3)	2970.8 (11.1)	2992.1 (9.1)	

consistent with the analysis of the NEXAFS spectra, and indicates that the C–C bond is strongest on the C(100)-2 × 1 surface, and weakest on Si(100)-2 × 1.

The IR spectra of benzene adsorbed on the surface shows two C–H stretching bands arising from the the sp<sup>2</sup> hybridized carbon atoms not bonded to the surface and sp<sup>3</sup> carbon atoms bonded directly to the surface. The vibrational frequencies for the C–H stretching modes of the sp<sup>3</sup> carbon atoms is computed to lie at approximately 2971 cm<sup>-1</sup>, compared to an experimental value of 2945 cm<sup>-1</sup> [26]. For the sp<sup>2</sup> carbon atoms, the C–H stretching band is predicted to lie at approximately 3063 cm<sup>-1</sup>, compared to an experimental value of 3044 cm<sup>-1</sup> [26]. Both of the predicted frequencies are a little too high, this may be a consequence of the cluster model of the surface used will not capture the interaction between the adsorbed molecule and the extended surface. The predicted vibrational frequencies for the sp<sup>2</sup> carbons do not vary significantly between the three surfaces. For the sp<sup>3</sup> carbons that are bonded directly to the surface, the predicted frequencies increase in the order C(100)-2 × 1 < Si(100)-2 × 1 < Ge(100)-2 × 1. The magnitude of the difference in frequencies between Si(100)-2 × 1 and Ge(100)-2 × 1 is approximately 20 cm<sup>-1</sup>, which is a little greater than the 15 cm<sup>-1</sup> observed for butadiene. The calculations indicate a decrease in frequency for the C(100)-2 × 1 surface compared with the Si(100)-2 × 1 surface, which contrasts with acetylene for which an increase in the C–H stretching frequencies is predicted.

#### 4. Conclusions

DFT calculations of the NEXAFS and IR spectroscopy of acetylene and benzene have been described. Within TDDFT, core excitation energies computed with a modified hybrid exchange-correlation functional with an increased fraction of HF exchange are in good agreement with values measured in experiment. Although it should be noted that this functional has been optimized for carbon 1s excitations, and a different fraction of HF exchange would be optimal for other types of core excitation. For acetylene, the π\* excitation energy is dependent on the nature of the underlying surface, and correlate with the length of the C–C bond length of the adsorbed molecule with a shorter bond leading to a higher excitation energy. For benzene, π\* orbitals are associated with carbon atoms that are not bond directly to the surface, and no significant variation of the excitation energy between the surfaces is predicted. Weaker features at higher energy arising for σ<sub>C–H</sub>\* and σ<sub>X–C</sub>\* excitations are also predicted. These bands show a similar behavior for acetylene and benzene. The σ<sub>C–H</sub>\* shows little dependence on the surface, while the σ<sub>X–C</sub>\* band is much higher for the C(100)-2 × 1 surface than both Si(100)-2 × 1 and Ge(100)-2 × 1 surfaces, reflecting the greater strength of the adsorbate-surface bond.

Calculations of the IR spectra show the C–H stretching frequencies for carbon atoms bonded directly to the surface have significant variations between the three surfaces. The frequencies are predicted to be 4–20 cm<sup>-1</sup> higher on the Ge(100)-2 × 1 surface compared to the Si(100)-2 × 1 surface. For acetylene, an increase in frequency is predicted, while for benzene a decrease in frequency is predicted for the C(100)-2 × 1 surface compared to the Si(100)-2 × 1 surface. Overall, DFT calculations can provide an accurate description of the NEXAFS and IR spectra of these systems, and can be a useful tool to aid the interpretation of experiment.

#### Acknowledgements

F.A.A. would like to acknowledge the Papua Government for a Ph.D. studentship grant. The authors are also grateful to the Uni-

versity of Nottingham for access to its high performance computing facility.

#### References

- [1] S.F. Bent, Surf. Sci. 500 (2002) 879.
- [2] R. Konecny, D.J. Doren, J. Am. Chem. Soc. 119 (1997) 11098.
- [3] R. Konecny, D.J. Doren, Surf. Sci. 417 (1998) 169.
- [4] A.V. Teplyakov, M.J. Kong, S.F. Bent, J. Chem. Phys. 108 (1998) 4599.
- [5] P. Moriarty, M.D. Upward, A.W. Dunn, Y.-R. Ma, P.H. Beton, D. Teehan, Phys. Rev. B 57 (1998) 362.
- [6] K. Sakamoto, D. Kondo, M. Hirada, A. Kimura, A. Kakizaki, S. Suto, Surf. Sci. 433–435 (1999) 642.
- [7] D. Kondo, K. Sakamoto, H. Takeda, F. Matsui, K. Amemiya, T. Ohta, W. Uchida, A. Kasuya, Surf. Sci. 514 (2002) 337.
- [8] R.J. Hamers, S.K. Coulter, M.D. Ellison, J.S. Hovis, D.F. Padowitz, M.P. Schartz, C.M. Greenlief, J.N. Russell Jr., Acc. Chem. Res. 33 (2000) 617.
- [9] L.A. Curtiss, M.S. Gordon (Eds.), Computational Materials Chemistry-Methods and Applications, Kluwer Academic Publishers, Dordrecht, Boston, London, 2004.
- [10] A.V. Teplyakov, P. Lal, Y. Noah, S.F. Bent, J. Am. Chem. Soc. 120 (1998) 7377.
- [11] P. Lal, A.V. Teplyakov, Y. Noah, M.J. Kong, G.T. Wang, S.F. Bent, J. Chem. Phys. 110 (1999) 10545.
- [12] Q. Liu, R. Hoffmann, J. Am. Chem. Soc. 117 (1995) 4082.
- [13] Y. Imamura, Y. Morikawa, T. Yamasaki, H. Nakatsuji, Surf. Sci. 341 (1995) L1091.
- [14] D. Sorescu, K.D. Jordan, J. Phys. Chem. B 104 (2000) 8259.
- [15] J.M. Rintelman, M.S. Gordon, J. Phys. Chem. B 108 (2004) 7820.
- [16] Y. Jung, M.S. Gordon, J. Am. Chem. Soc. 127 (2005) 3131.
- [17] J.-H. Cho, K.S. Kim, Y. Morikawa, J. Chem. Phys. 124 (2006) 024716.
- [18] M. Sternberg, P. Zapol, L.A. Curtiss, Phys. Rev. B. 68 (2003) 205330.
- [19] P. Zapol, L.A. Curtiss, H. Tamura, M.S. Gordon, in: L.A. Curtiss, M.S. Gordon (Eds.), Computational Materials Chemistry-Methods and Applications, Kluwer Academic Publishers, Dordrecht, Boston, London, 2004, p. 266.
- [20] M. Sternberg, P. Zapol, L.A. Curtiss, Mol. Phys. 103 (2005) 1017.
- [21] M. Sternberg, D.A. Horner, P.C. Redfern, P. Zapol, L.A. Curtiss, J. Comput. Theor. Nanosci. 2 (2005) 207.
- [22] H. Tamura, M.S. Gordon, Chem. Phys. Lett. 406 (2005) 197.
- [23] F. Matsui, H.W. Yeom, A. Imanishi, K. Isawa, I. Matsuda, T. Ohta, Surf. Sci. Lett. 401 (1998) L413.
- [24] F. Matsui, H.W. Yeom, I. Matsuda, T. Ohta, Phys. Rev. B 62 (2000) 5036.
- [25] A. Pietzsch, F. Hennies, A. Föhlisch, W. Wurth, M. Nagasono, N. Witkowski, M.N. Piancastelli, Surf. Sci. 562 (2004) 65.
- [26] M.J. Kong, A.V. Teplyakov, J.G. Lyubovitsky, S.F. Bent, Surf. Sci. 411 (1998) 286.
- [27] N. Witkowski, F. Hennies, A. Pietzsch, S. Mattsson, A. Föhlisch, W. Wurth, M. Nagasono, M.N. Piancastelli, Phys. Rev. B 68 (2003) 115408.
- [28] K. Newstead, A.W. Robinson, S. d'Addato, A. Patchett, N.P. Prince, R. McGrath, R. Whittle, E. Dudzik, I.T. McGovern, Surf. Sci. 287–288 (1993) 317.
- [29] A. Hoffmann, G. Comtet, L. Hellner, G. Dujardin, M. Petracic, Appl. Phys. Lett. 73 (1998) 1152.
- [30] N.A. Besley, A. Noble, J. Phys. Chem. C 111 (2007) 3333.
- [31] Y. Taguchi, M. Fujisawa, T. Takoka, T. Okada, M. Nishijima, J. Chem. Phys. 95 (1991) 6870.
- [32] G.P. Lopinski, T.M. Fortier, D.J. Moffatt, R.A. Wolkow, J. Vac. Sci. Technol. 16 (1998) 1037.
- [33] B. Naydenov, W. Widdra, J. Chem. Phys. 127 (2007) 154711.
- [34] G.T. Wang, C. Mui, C.B. Musgrave, S.F. Bent, J. Phys. Chem. B 103 (1999) 6803.
- [35] C. Mui, G.T. Wang, S.F. Bent, C.B. Musgrave, J. Chem. Phys. 114 (2001) 10170.
- [36] K.T. Nicholson, M.M. Banaszak Holl, Phys. Rev. B 64 (2001) 155317.
- [37] M.A. Phillips, N.A. Besley, P.M.W. Gill, P. Moriarty, Phys. Rev. B 67 (2003) 035309.
- [38] K. Okamura, H. Ishii, Y. Kimuar, M. Niwano, Surf. Sci. 576 (2005) 45.
- [39] N.A. Besley, J.A. Bryan, J. Phys. Chem. C 112 (2008) 4308.
- [40] M. Stener, G. Fronzoni, M. de Simone, Chem. Phys. Lett. 373 (2003) 115.
- [41] S. Hirata, M. Head-Gordon, Chem. Phys. Lett. 314 (1999) 291.
- [42] A. Dreuw, M. Head-Gordon, Chem. Rev. 1005 (2005) 4009.
- [43] N.A. Besley, Chem. Phys. Lett. 390 (2004) 124.
- [44] F.A. Asmuruf, N.A. Besley, J. Chem. Phys. 129 (2008) 064705.
- [45] N.A. Besley, J. Chem. Phys. 122 (2005) 184706.
- [46] N.A. Besley, A.J. Blundy, J. Phys. Chem. B 110 (2006) 1701.
- [47] A. Nakata, Y. Imamura, H. Nakai, J. Chem. Phys. 125 (2006) 064109.
- [48] A. Nakata, Y. Imamura, H. Nakai, J. Chem. Theor. Comput. 3 (2007) 1295.
- [49] A.D. Becke, Phys. Rev. A 28 (1988) 3098.
- [50] P.A.M. Dirac, Proc. Camb. Philol. Soc. 26 (1930) 376.
- [51] C. Lee, W. Yang, R.G. Parr, Phys. Rev. B 37 (1988) 785.
- [52] S.H. Vosko, L. Wilk, M. Nusair, Can. J. Phys. 58 (1980) 1200.
- [53] J.-H. Cho, L. Kleinman, J. Chem. Phys. 119 (2003) 2820.
- [54] N.A. Besley, K.A. Metcalf, J. Chem. Phys. 126 (2007) 035101.
- [55] N.A. Besley, Philos. Trans. R. Soc. 365 (2007) 2799.
- [56] A.P. Scott, L. Radom, J. Phys. Chem. 100 (1996) 16502.
- [57] Y. Shao, L. Fusti-Molnar, Y. Jung, J. Kussman, C. Ochsenfeld, S.T. Brown, A.T.B. Gilbert, L.V. Slipchenko, S.V. Levchenko, D.P. O'Neill, R.A. Distasio Jr., R.C.

Lochan, T. Wang, G.J.O. Beran, N.A. Besley, J.M. Herbert, Y.L. Lin, T. Van Voorhis, S.H. Chien, A. Sodt, R.P. Steele, V.A. Rassolov, P.E. Maslen, P.P. Korambath, R.D. Adamson, B. Austin, J. Baker, E.F.C. Byrd, H. Daschle, R.J. Doerksen, A. Dreuw, B.D. Dunietz, A.D. Dutoi, T.R. Furlani, S.R. Gwaltney, A. Heyden, S. Hirata, C.-P. Hsu, G. Kedziora, R.Z. Khaliullin, P. Klunzinger, A.M. Lee, M.S. Lee, W. Lian, I.

Lotan, N. Nair, B. Peters, E.I. Proynov, P.A. Pieniazek, Y.M. Rhee, J. Ritchie, E. Rosta, C.D. Sherrill, A.C. Simmonett, J.E. Subotnik, H.L. Woodcock III, W. Zhang, A.T. Bell, A.K. Chakraborty, D.M. Chipman, W.J. Hehre, A. Warshel, H.F. Schaefer III, J. Kong, A.I. Krilov, P.M.W. Gill, M. Head-Gordon, *Phys. Chem. Chem. Phys.* **8** (2006) 3172.